Kirk-Othmer Encyclopedia of Chemical Technology.

ZONE REFINING

Zone refining is one of a class of techniques known as fractional solidification, in which a separation is brought about by crystallization of a melt without solvent being added (see also Crystallization) (1–8). Solid–liquid phase equilibria are utilized, but the phenomena are much more complex than in separation processes utilizing vapor–liquid equilibria. In most of the fractional-solidification techniques described in the article on crystallization, small separate crystals are formed rapidly in a relatively isothermal melt. In zone refining, on the other hand, a massive solid is formed slowly and a sizable temperature gradient is imposed at the solid–liquid interface.

Zone refining was developed in the early 1950s at Bell Telephone Laboratories in response to the need for extremely pure germanium. It was an essential step for the development of the transistor and thus for the entire electronics revolution. Before that time, purification was carried out by normal freezing, also called progressive freezing. A melt was slowly frozen, causing more impurities to be concentrated in the last melt to freeze. In progressive freezing, however, a single solidification did not give sufficient purification. Simply remelting the entire ingot would redistribute the impurities, thereby eliminating the purification of the first solidification. the impure end could be removed, but handling and cutting introduce new impurities. The problem was solved by melting only a small part of the material and passing this molten zone down the ingot. Subsequent zone passes increased purification without requiring handling or cutting or permitting excessive back-mixing.

Zone refining can be applied to the purification of almost every type of substance that can be melted and solidified, eg, elements, organic compounds, and inorganic compounds. Because the solid–liquid phase equilibria are not favorable for all impurities, zone refining often is combined with other techniques to achieve ultrahigh purity.

The high cost of zone refining has thus far limited its application to laboratory reagents and valuable chemicals such as electronic materials. The cost arises primarily from the low processing rates, handling, and high energy consumption owing to the large temperature gradients needed.

Actually, zone refining is only one of a class of techniques known as zone melting in which a molten zone is passed down a solid rod. Zone melting is used routinely to collect impurities in high purity materials, eg, silicon, in preparation for chemical analysis. Growth of bulk single crystals is an important application that includes commercial float-zoning of silicon crystals for the semiconductor industry (7). Floating-zone melting is being considered for use aboard the U.S. Space Shuttle because the absence of gravity might permit larger crystals to be grown with greater homogeneity.

Addition of solvent to the zone allows crystals to be grown that either decompose before melting (incongruent melting) or have a very high vapor pressure at the melting point. This technique has been called both temperature-gradient zone melting and the traveling-heater method of crystal growth. It has also been used for fabrication of semiconductor devices (9).

Continuous zone-refining techniques have been developed, both theoretically and experimentally (1, 4, 10, 11).

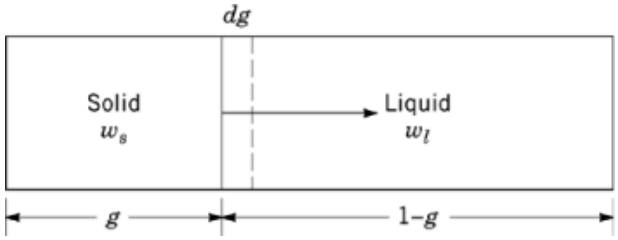

Fig. 1. Solidification of differential mass fraction dg of a melt. Mass fraction of impurity in melt is w_l and in solid freezing out is w_s (g).

1. Theory

Early zone-refining theory attempted to correlate the concentration of impurities with location.

1.1. Progressive Freezing

Although a rod geometry is not required, directional solidification in the Bridgman configuration is easiest to visualize. It is widely used for single-crystal growth and preparation of dendritic and eutectic composite materials.

To derive the concentration profile for progressive freezing, a material balance is employed for solidification of a small fraction dg of melt, as shown in Figure 1. Integration from the beginning of solidification gives (1, 4, 8):

$$\int_o^g (1-g)^{-1}\,dg = -\ln(1-g) = \int_{w_o}^{w_l} (w_l - w_s)^{-1}\,dw_l \qquad (1)$$

where g is mass fraction already solidified, w_o is the original mass fraction of impurity, w_s is the mass fraction of impurity in the solid at g, and w_l is the average impurity concentration in the liquid melt. It has been assumed that no mass transfer occurs in the solid, which is nearly always true because of the absence of convective mixing and the very low diffusion coefficients. Without solid-state diffusion, the solid, once it is formed, does not know the melt is there. This is analogous to batch evaporation with the removal of the vapor as it forms.

In order to integrate equation 1, it is necessary to have a relationship between w_l and w_s. If there is equilibrium between the bulk melt and the solid freezing out, phase-diagram data may be used. As shown in Figure 2, in the limit of very small impurity contents, w_s is often proportional to w_l, ie, $w_s = kw_l$ where k is the distribution or segregation coefficient. Equation 1 may then be integrated:

$$w_s/w_o = k(1-g)^{k-1} \qquad (2)$$

This relationship is plotted in Figure 3 for several values of k; for $k < 1$ (the usual situation for impurities), $w_s \longrightarrow \infty$ as $g \longrightarrow 1$. Clearly, this assumption cannot be correct; w_s is no longer proportional to w_l at high concentrations.

1.2. Zone Melting

A similar material balance may be made for a zone of mass m_z moving a short distance in such a manner that the mass dm of solid is frozen out and an identical mass melts into the zone (Fig. 4). For the first zone pass, it is assumed that the rod is initially at uniform composition w_o to obtain the following (1, 4, 8):

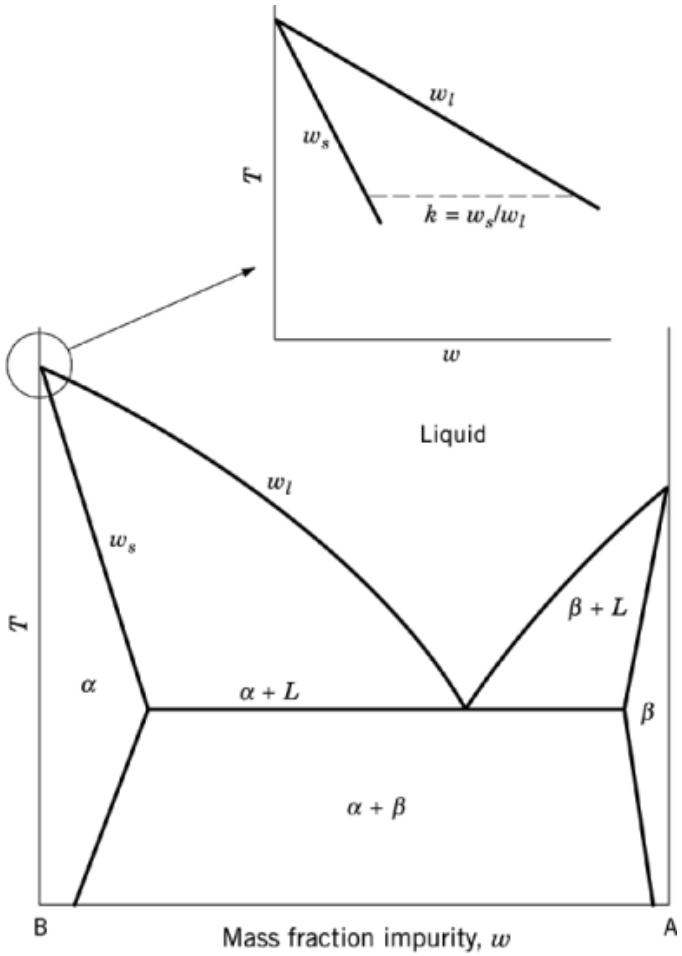

Fig. 2. Typical binary phase diagram for host and impurity, showing a constant distribution coefficient if impurity content is low. L=liquid composition after some solidification, α=B and small amount of A, β=A and small amount of B, w_l=liquidus, and w_s=solidus.

$$\int_o^m m_z^{-1} dm = m/m_z = \int_{w_o}^{w_l} (w_o - w_s)^{-1}\, dw_l \qquad (3)$$

For constant $k = w_s/w_l$, this may be integrated to yield

$$w_s = w_o \left[1 - (1 - k)\, \exp(-km/m_z)\right] \qquad (4)$$

Note that m/m_z is approximately the number of zone lengths down the rod.

Computations are more difficult for subsequent zone passes, since the starting composition of the rod is no longer uniform. Nevertheless, a variety of numerical and analytical results has been obtained for infinite and for finite rods (1, 4, 12–16). A typical result is shown in Figure 5. Substantial purification can be attained even when k is not significantly different from 1.

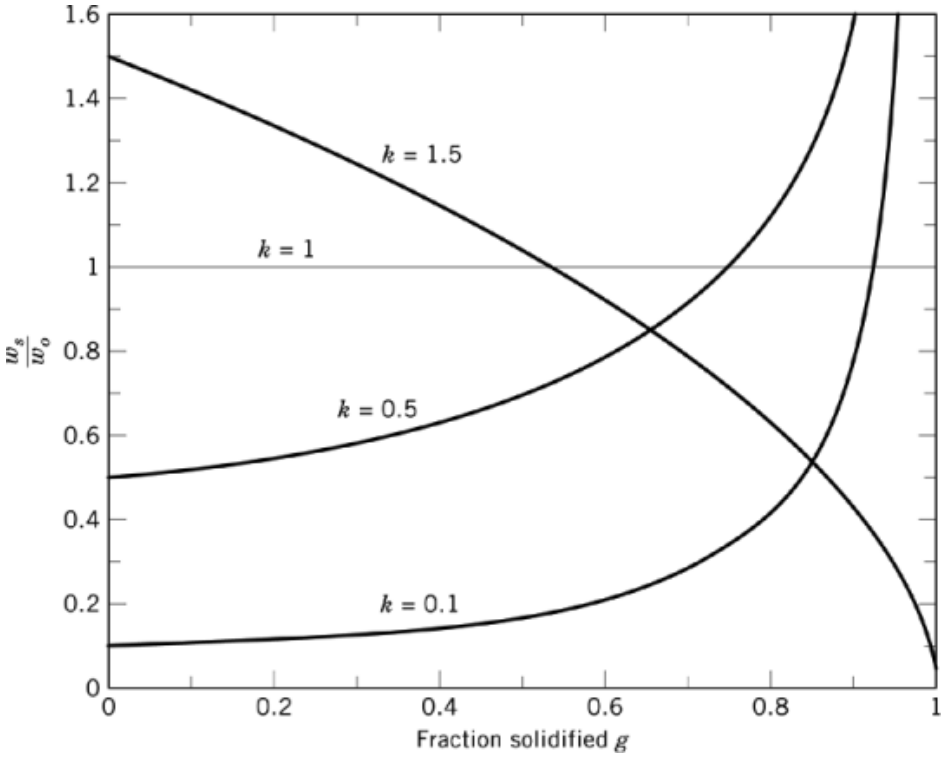

Fig. 3. Impurity concentration profiles resulting from progressive freezing with different values of distribution coefficient k (from eq. 2).

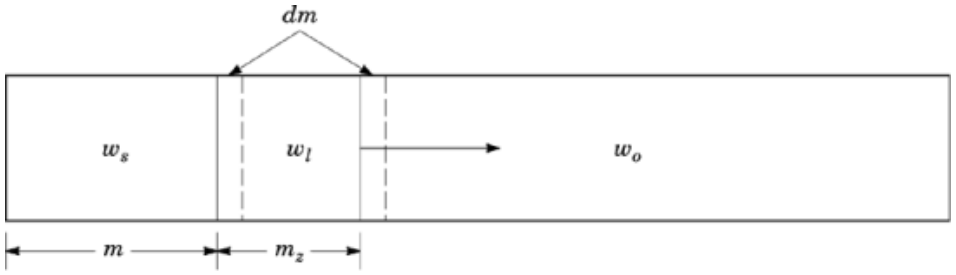

Fig. 4. Movement of molten zone by differential amount dm for initial zone pass; original solid has uniform impurity content w_o.

With subsequent zone passes, back-mixing becomes increasingly significant. When the number of zone passes becomes very large, the concentration profile reaches the ultimate distribution and subsequent passes have no influence. The number of zone passes required to approach the ultimate distribution is about twice the number of zone masses in the rod for small effective distribution coefficients. Thus, longer zones permit the attainment of the ultimate distribution sooner. On the other hand, the attainable separation increases as the zone size becomes smaller (permitting less back-mixing) (1, 4).

Although most impurities have $k < 1$, there are exceptions, and it cannot be automatically assumed that the purest material is at the front end of the ingot; sometimes it is in the middle.

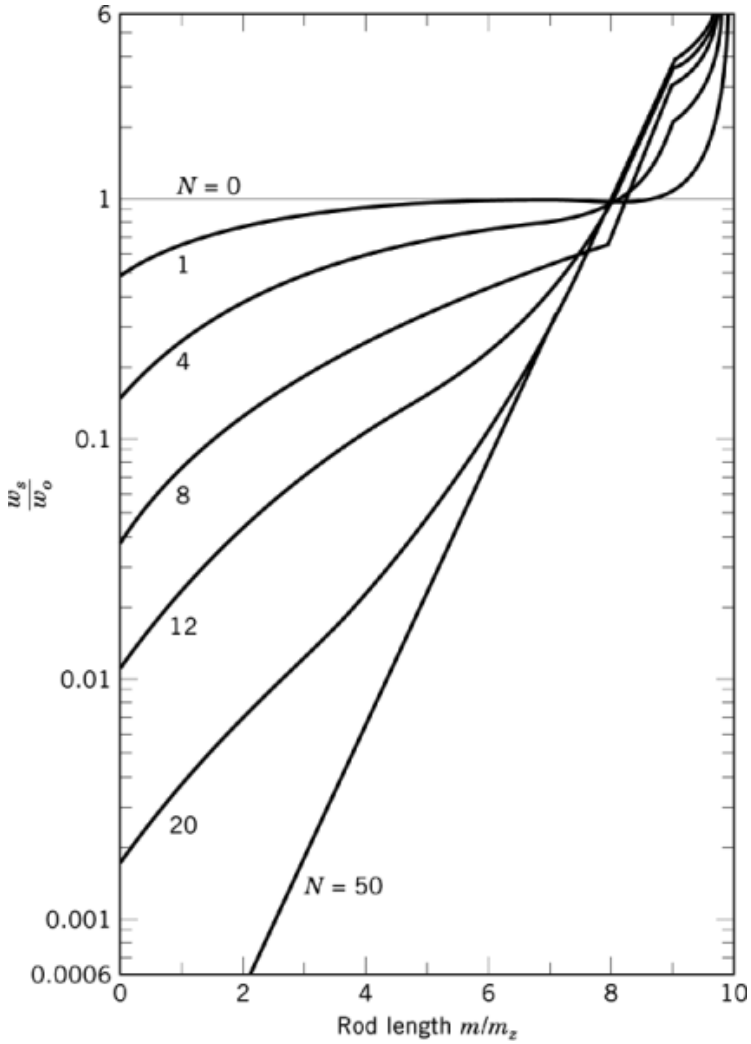

Fig. 5. Concentration profiles for different numbers N of zone passes for k=0.5 and a rod containing 10 zone masses. Obtained by numerical methods of ref. 13 using Texas Instruments 99/4 Home Computer.

Theoretical treatments have also been given to other situations of interest. In zone leveling, the impurity level is homogenized either by moving the zone back and forth along a linear rod, or by movement around a ring (1). Evaporation and condensation of a volatile impurity (17, 18), as well as decomposition of the material itself (13), have also been treated.

1.3. Nonideal Separations

In numerous instances, the ideal equations 2 and 4 have been verified experimentally. However, in other experiments different results were obtained, reflecting failure of one ore more of the assumptions made in deriving equations 2 and 4. Likewise, much theoretical work is concerned with modified assumptions, including

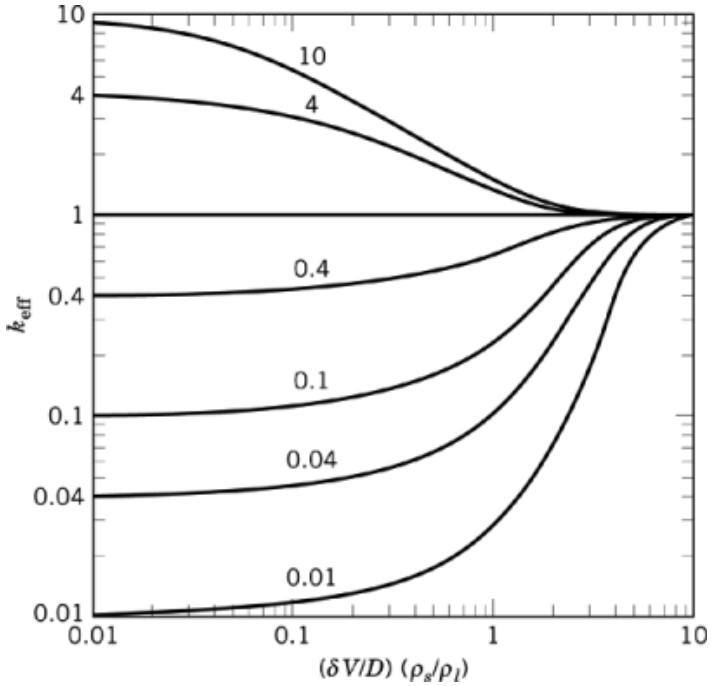

Fig. 6. Effective distribution coefficient k_{eff} vs interfacial distribution coefficient k and dimensionless zone-travel velocity; $k_{\text{eff}}$is to be used in place of k in expressions for concentration profiles, such as equations 2 and 4.

varying distribution coefficient k (19), eutectic-forming phase behavior (4, 20, 21), varying mass m_z of zone (22), and solid-state diffusion (23).

The assumption of equilibrium between solid w_s and bulk melt w_l is frequently violated because of lack of complete mixing in the melt. A steady-state fictitious stagnant-film treatment may be employed to arrive at an effective distribution coefficient,

$$k_{\text{eff}} \equiv \frac{w_s}{w_l} = \frac{k}{k + (1-k)\ \exp\left(-\delta V \rho_s / D\rho_l\right)} \qquad (5)$$

where k is the equilibrium distribution coefficient from the phase diagram, δ is the film thickness (erroneously called the boundary-layer thickness), V the linear freezing rate, ρ_s the density of the solid, D the binary diffusion coefficient in the melt, and ρ_l the density of the liquid (1, 4, 5, 24–26). The film thickness δ is related to the mass-transfer coefficient k_c and the Sherwood number N_{Sh} by

$$\delta = D/k_c = L/Sh \qquad (6)$$

It has been found to be only weakly dependent on V (25). As shown in Figure 6, equation 5 predicts that $k_{\text{eff}} \longrightarrow k$ as $V \longrightarrow 0$, and $k_{\text{eff}} \longrightarrow 1$ as $V \longrightarrow \infty$. Thus, the separation obtained diminishes as the zone travel rate increases.

In practice, the freezing rate V is rarely constant. Fluctuating convective currents in the melt (27–32) lead to a fluctuating freezing rate, which causes k_{eff} to be somewhat nearer unity than predicted by equation 5. A fluctuating freezing rate also leads to impurity striations, ie, bands of varying impurity content parallel

to the freezing interface. Irregular free convection in liquid metals has been damped successfully by means of a constant magnetic field, about 0.4 T (4 kG) for a melt of 1 cm dia (27, 33–36).

The equilibrium distribution coefficient k varies with distance down the ingot because of compositional stress in the crystal (37, 38), departure from linearity on the phase diagram at large impurity concentrations, and interactions with other impurities. The actual interfacial-distribution coefficient k_i can depart from equilibrium because of adsorption on the growing interface (5, 39, 40), differences in incorporation kinetics of impurity and host atoms (41–43), and interface-field effects (44). Deviation of k_i from k in such cases increases as the growth velocity V increases. For $k < 1$, k_i can even exceed 1 at moderate V. The well-known facet effect generally is thought to arise from such phenomena, and k_i is much greater on the faceted portion of the interface than on a nonfaceted part of the same interface (4, 5).

As the zone-travel rate is increased, a breakdown of the freezing interface from smooth to dendritic is eventually observed. Dendrites are treelike structures that trap melt and dramatically reduce separation. The onset of interface breakdown is predicted by the elementary theory of constitutional supercooling (1, 4, 5). As shown in Figure 7**a**, $k < 1$ causes impurity to accumulate in the melt at the freezing interface, thereby lowering the freezing point. Thus, the actual temperature may be below the melting point for some distance into the melt, even though the two are identical at the freezing interface (see Fig. 7**b**). This is known as constitutional supercooling because it is brought about by a change in constitution or composition. The interface is unstable with respect to perturbation in shape, and cells or dendrites are expected.

At the onset of constitutional supercooling, the melting-point gradient exceeds the temperature gradient. Equating these gradients leads to the criterion for constitutional supercooling:

$$V/G > D\rho_l/(\partial T_e/\partial w_i)\,\rho_s(w_s - w_i) = Dk\rho_l/(\partial T_e/\partial w_i)\,\rho_s w_s(k-1)$$

$$= D\rho_l\left[k + (1-k)\,\exp(-\delta V\rho_s/\rho_l D)\right]/(\partial T_e/\partial w_i)\,\rho_s(k-1)\,w_l \qquad (7)$$

where G is the imposed interfacial-temperature gradient and $\partial T_e/\partial w_i$ is the slope of the liquidus on the phase diagram (change of freezing point with impurity concentration). Much more advanced and complicated treatments of morphological stability have been made (45–54). However, most experimental results are adequately predicted by the constitutional-supercooling theory outlined here (55–57).

From equation 7, it may be seen that the tendency toward constitutional supercooling increases as the freezing rate V increases, the temperate gradient G decreases, the impurity content w increases, the separation $(w_s - w_i)$ between liquidus and solidus in the phase diagram increases, and the stirring decreases (δ increases). This explains why zone melting is limited to purification of materials with low impurity contents, and why substantial temperature gradients and low zone-travel rates are necessary.

Under the microscope, the onset of constitutional supercooling first manifests itself by the formation of a grooved interface, rather than dendrites. Dendritic growth occurs at higher freezing rates. In strongly faceted materials (high entropy of fusion), needles and plates may occur rather than branched dendrites. The separation is reduced whenever the interface is no longer smooth. Nevertheless, k_{eff} does not become precisely one even with severely dendritic growth, ie, some separation still occurs (58–61).

Insoluble particles may also be removed during zone refining. Most particles are pushed by a freezing solid–liquid interface, provided that the freezing rate is sufficiently slow. In the absence of stirring, a particle is pushed up to a critical freezing rate V_c, beyond which it is trapped (62–65). The critical freezing rate is roughly inversely proportional to the particle size for smooth particles and less dependent on particle size for rough particles. For 15-μm diameter smooth spheres, V_c is about 10 mm/h.

Stirring dramatically enhances separation of foreign particles by zone melting. If the particles are not allowed to rest on the freezing interface, they are pushed at much larger velocities than V_c in the absence of

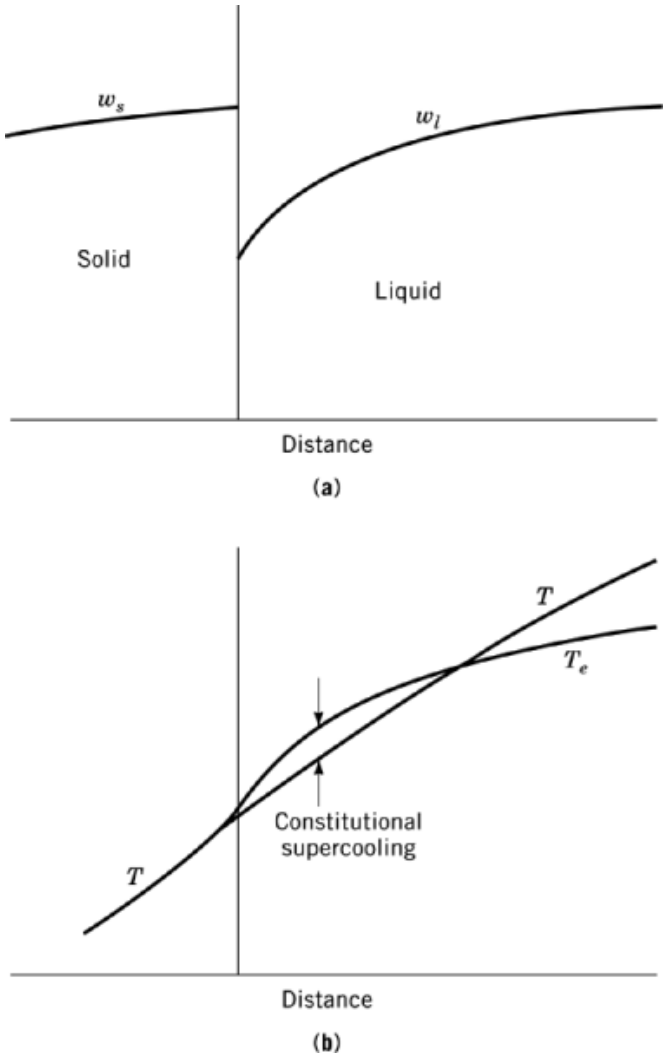

Fig. 7. Constitutional supercooling. (**a**) impurity concentration profile during solidification; (**b**) actual temperature T and equilibrium freezing temperature T_e during solidification.

stirring, although there is no sharp demarcation velocity between pushing and engulfment. The probability of trapping increases as particle size and stirring decrease and the amount of particles increases (66, 67).

A variety of other phenomena influence fractional solidification of organic compounds (68).

1.4. Optimization

Zone travel rate, sample geometry and orientation, zone length and spacing, stirring in the zone, and the number of zone passes can all be controlled. These variables can be optimized either with respect to purification or to the purification rate.

For maximum purification, the zone should move as slowly as possible, the sample should be many zone lengths long, the melt should be stirred, and more zone passes should be made than several times the number

of zone lengths in the sample. Stirring and slow zone travel lower $\delta V/D$, which in turn increases $|1 - k_{\text{eff}}|$, as shown by equation 5 and Figure 6. In practice, it is sufficient for $\delta V/D \lesssim 0.1$.

Stirring is essential to maximize the rate of purification, and the travel rate V should be adjusted in such a way that $\delta V/D \approx 1$ (1, 4). In addition, the narrow zones should be as close together as possible, a rod should be only about 10 zone lengths long, and there should be about as many zone passes as there are zone lengths in the rod. In the absence of tube rotation, heat transfer limits the minimum zone length and zone spacing to approximately the sample diameter, which is typically about 1 cm. The value $\delta V/D \approx 1$ derives from a consideration of equation 5, which is only valid in the absence of constitutional supercooling. In no case should the zone be moved so fast that dendritic growth occurs. Thus, whenever possible, the freezing interface should be examined with a microscope during zoning (69).

Dendritic growth can be avoided by keeping the zone travel rate low for the first few passes. As impurity is removed (for $k < 1$), higher zoning rates are possible. If dendritic growth is not a problem, $\delta V/D \approx 1$ at the beginning, followed by a gradual decrease of V for subsequent passes, in order for $|1 - k_{\text{eff}}|$ to increase. Otherwise, the possible ultimate purification is limited, and the purification rate of later zone passes is low.

Since the separation occurs at the solid–liquid interface, the purification rate is maximized by having many zones close together. If this is not possible and only one zone can be passed at a time, the rate is maximized by having the first zone as long as possible and decreasing the length of subsequent zones.

2. Equipment and Techniques

2.1. Containers

The ideal container for zone melting should not contaminate the melt nor be damaged by the melt or subsequent contraction of the solid. For organic materials, borosilicate glasses are especially suitable, although metals and fluorocarbon and other polymers have also been successfully employed.

For many metals and semiconductors, fused silica (often erroneously called quartz) is ideal (5). Sometimes, the substance sticks to the glass and causes a break. Such breakage is prevented by coating the inside of the vessel with a film of carbon, conveniently deposited by passing acetone vapor through the glass tube at ca 700°C. However, at high temperatures such coating may result in contamination with carbon or silicon. Metals such as aluminum, with a high free energy of oxidation, react with silica glasses. In such cases, an oxide container of still higher free energy of formation is used, such as alumina or even sapphire. Zirconia and boron nitride have also been employed.

High melting inorganic salts and oxides are conveniently, albeit expensively, treated in noble-metal containers, platinum, rhodium, and iridium. Refractory containers, such as graphite, molybdenum, and tungsten in inert atmospheres, are also successfully employed for such salts. Low melting salts are refined in fused silica. Glassy carbon and pyrolytic graphite are good substitutes for ordinary graphite when carbon particles are a problem.

It is prudent to perform zone melting in a dry inert atmosphere. Oxygen causes most organic melts to oxidize slowly. Oxygen and moisture not only oxidize metals and semiconductors, but often enhance sticking to the container. Molten salts attack silica more rapidly in the presence of moisture. Oxygen and water are considered impurities in some inorganic compounds.

Moisture is removed from fused silica by heating, preferably in vacuum. Prior to this, silica ampuls are sometimes rinsed with a detergent solution, hydrofluoric acid, nitric acid, or methanol. After cleaning, drying, and loading, the ampul may be alternately evacuated and back-filled with inert gas. Sealing is easier if the inert-gas pressure is only slightly below atmospheric.

The container may either be in the form of a tube or a horizontal boat. A boat is advantageous for removal of the substance after zone melting, but may not be feasible if the substance is volatile. Most organic compounds,

for example, are too volatile to be zone refined in an open boat. After zone melting, a silica glass ampul may be removed by etching with hydrofluoric acid, carefully cutting lengthwise with a diamond saw, or tapping with a ball-peen hammer to propagate cracks.

Because the solid and melt differ in density, repeated zone passes can transport material along the container. If the substance expands upon melting, it tends to travel toward the front, and vice versa. With a horizontal boat, this can be avoided by tilting. The tilt can be adjusted in such a way that whenever a zone reaches the end of the ingot some melt overflows, thereby removing some impurity and preventing back mixing upon subsequent zone passes. Precautions must be taken with a sealed tube to prevent rupture of the container caused by material transport. With organic compounds that expand upon melting, provisions must be made for this expansion when the zone forms at the front end of the ampul by leaving an empty space at the front end, separated from the substance by a fluorocarbon polymer plug. Each time a new zone is formed, the plug is forced to move to take up the expansion.

2.2. Drive Mechanisms

Either the heaters or the sample may be moved. The optimal zone travel rates are typically rather slow, ie, ca 1 cm/h. Thus, electric-motor drives require gearing systems, resulting in an undesirably jerky stick-slip movement. This is avoided with double-rod supports with linear ball bearings and with low backlash gears, where tension on the moving piece pushes in the direction of motion. To ensure a smooth drive, it is useful to take time-lapse films during zoning. Even with the most stringent precautions, both low level mechanical-drive fluctuations and temperature fluctuations persist, and a zone-travel rate $>1\ \mathrm{mm/h}$ is generally not considered practical. If constitutional-supercooling problems require a rate below this, other purification methods are preferable.

Pneumatic and hydraulic drive systems have also been used, although not widely.

If many zones are present in the sample simultaneously, it may be advantageous to move the ampul (or heaters) slowly by one zone spacing, and then rapidly backward to catch the next zone. By such a reciprocating action, many zones can be moved continuously through the sample without a bank of heaters longer than the sample.

2.3. Heating and Cooling

Heat must be applied to form the molten zones, and this heat much be removed from the adjacent solid material (4, 70). In principle, any heat source can be used, including direct flames. However, the most common method is to place electrical resistance heaters around the container. In air, nichrome wire is useful to ca 1000°C, Kanthal to ca 1300°C, and platinum-rhodium alloys to ca 1700°C. In an inert atmosphere or vacuum, molybdenum, tungsten, and graphite can be used to well over 2000°C.

Conductors can be heated to very high temperatures by induction heating wherein the sample is surrounded by a water-cooled coil carrying high current at high frequencies. A frequency of 450 kHz is typical for good conductors with a diameter $>1-2\ \mathrm{cm}$. Floating-zone melting requires frequencies of several MHz. Basically, the high frequency electromagnetic field induces a current within the sample itself, which is then heated by the resistance losses. The lower the frequency and the lower the electrical resistance, the deeper the field penetrates. Contact with the specimen is not required, and there are no limits to the temperatures attainable. If the substance is not a conductor, it is still possible to use induction heating. A conducting ring, eg, graphite, is place between the sample and the high frequency coil. This susceptor is heated by the field, and in turn transmits heat to the sample by radiation, conduction, and convection.

Molten zones are also formed by radiant heating (71). The light source may be focused carbon arcs, xenon lamps, sunlight, or lasers. Very high temperatures have been achieved with all of these. For example, sapphire has been float-zoned in this manner, at over 2000°C.

An electron beam can be used for floating-zone melting of a conducting rod. For example, a heated tungsten ring is placed around the zone in a vacuum and made strongly negative. Electrons are emitted from the tungsten and deliver the entire voltage-drop energy to the zone. A positive connection is made to the end of the rod to drain the current.

Electric heaters have also been directly immersed in the molten zone. Zone refining has been accomplished with a single helical heater rotating in an annular sample space (71).

It is important to control temperature and power input of the heaters. A fluctuating heat input leads to a fluctuating freezing rate, thereby reducing separation. It can also cause breakage of the container because $\rho_l \neq \rho_s$. A variable autotransformer (eg, Powerstat or Variac) fed by a constant voltage transformer (eg, Sola) affords a convenient and cheap source of energy. The voltage is increased until the zone is the desired size. An oversized constant-voltage transformer does not give constant voltage. It is not necessary to actually know the temperature anywhere in the system.

Heat is often removed by simply allowing it to escape by convection, radiation, and conduction. However, such uncontrolled escape can lead to very large temperature fluctuations. It is better to surround the entire container, heaters and all, with a controlled-temperature cooled chamber. Even then, buoyancy-driven free convection from the ampul can lead to small temperature fluctuations. Jets of air or cooling water applied directly onto the ampul adjacent to the heater have been employed. Both temperature and flow rate of the coolant should be controlled.

2.4. Floating-Zone Melting

No completely satisfactory container material exists for many high melting materials. In such cases, floating-zone melting may be employed (1, 5, 7). Heat is applied to a vertical rod, usually by induction, electron-beam, or radiant methods. In early applications, the roughly cylindrical molten zone was held by surface tension, and rods of only a few mm in diameter could be zoned thereby. The demand for large-diameter silicon for semiconductor devices led to a modification. Typically, an induction-heating pancake coil is used with a diameter smaller than that of crystal. As shown in Figure 8, the upper feed rod melts to a conical shape, with the melt running down through the so-called eye-of-the-needle induction heating coil. The melt collects in a puddle and freezes onto the growing crystal below. The electromagnetic field of the induction heating coil supports the molten zone. In this way, dislocation-free single silicon crystals of >10 cm dia and almost 1 m long are grown commercially.

The primary application for floating-zone melting is crystal growth rather than purification. Semiconductor-grade silicon is not purified by zone refining; silicon chlorides are distilled and then reduced with hydrogen.

2.5. Stirring

As noted earlier, stirring increases the optimal zone-travel rate by lowering δ and aids significantly in removal of foreign particles. Even in the absence of stirring, convection motion occurs in the melt (27). In a vertical sealed ampul, the driving force is buoyancy, ie, the interaction of gravity with density gradients owing to temperature and compositional variations. If the zone is shorter than the heater and the impurity content is low, the most vigorous convection is along the top interface. If that were the sole consideration, the top interface should be the freezing interface, ie, the zone should be moved downward. However, a gas bubble frequently forms at the top of the zone caused by release of the gas bubbles trapped in the solid during the casting of the feed ingot. Material evaporates across the gas space at the top of the zone, leading to a dramatically altered separation. Furthermore, the processes of evaporation, condensation, freezing, and dripping of condensate back into the melt are so complicated that the separation is difficult to predict and may be irreproducible (68). Therefore, the zone is frequently moved up so that the freezing interface is on the bottom.

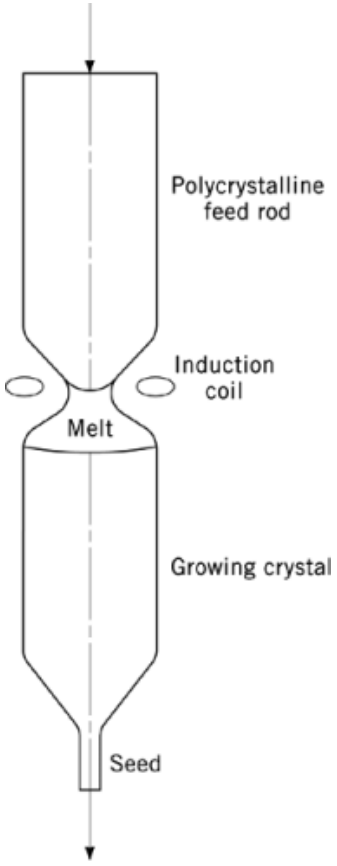

Fig. 8. Geometry for float-zoning large-diameter conducting materials.

The buoyancy-driven natural convection along the freezing interface in horizontal operation tends to be fairly vigorous. However, it also leads to spreading of the zone at the top owing to convection transport of heat upward.

With natural convection, δ is between 0.1 and several mm (4).

It is frequently very helpful to rotate the tube about its axis. In horizontal zone melting with a gas bubble along the top of the zone, rotation causes good stirring and enhances removal of foreign particles. Some insoluble particles are still trapped as long as the bubble contacts the freezing interface. Tilting the tube or making subsequent zone passes without a bubble can lead to virtually complete elimination of foreign particles. Although particles are very effectively removed if no gas bubble is present, δ is then about the same as with free convection (66, 67).

With vertical zone melting and horizontal zone melting without a gas bubble, simple tube rotation at a constant moderate velocity does not significantly influence δ. In those cases, accelerated crucible rotation or spin up–spin down could be used (72–75). The tube is spun more rapidly than described above, but not at constant velocity. It may, for example, be spun rapidly, suddenly stopped, spun rapidly, etc, resulting in very vigorous stirring.

In recent years, it has been shown theoretically and experimentally that surface-tension gradients can give rise to very vigorous stirring (76–80). A free melt-vapor surface is required, as with floating-zone melting

or horizontal processing in an open boat. Surface tension depends on temperature and composition, both of which vary along the melt surface. The surface moves from areas of low surface tension to areas of high surface tension, carrying the underlying melt along via viscosity. This is called Marangoni convection or thermocapillary convection. It occurs only if a surfactant does not immobilize the surface, which occurs surprisingly often. For example, most organic melts contain surfactant impurities which strongly inhibit Marangoni convection (81). Surface segregation also occurs in metal-alloy melts.

Induction heating is thought to cause vigorous convection because of the spatially varying average force field imposed along the melt surface.

Deliberate stirring can be imposed on conductors with a transverse rotating magnetic field or by passage of electric current axially with a transverse magnetic field. Conversely, a constant magnetic field with no current imposed greatly reduces natural convection.

Oscillators (82) and ultrasonic vibrations (83) have also been used to lower δ.

BIBLIOGRAPHY

"Zone Refining" in the *ECT* 2nd ed., Vol. 22, pp. 680–702, by Alan Lawley and D. Robert Hay, Drexel University; in *ECT* 3rd ed., Vol. 24, pp. 903–917, by W. R. Wilcox, Clarkson College of Technology.

Cited Publications

1. W. G. Pfann, *Zone Melting*, 2nd ed., John Wiley & Sons, Inc., New York, 1966.
2. E. F. G. Herington, *Zone Melting of Organic Compounds*, John Wiley & Sons, Inc., New York, 1966.
3. H. Schildknecht, *Zonenschmelzen*, Verlag Chemie, Weinheim, Germany, 1964.
4. M. Zief and W. R. Wilcox, *Fractional Solidification*, Marcel Dekker, Inc., New York, 1967.
5. J. C. Brice, *The Growth of Crystals from Liquids*, North-Holland Publishing Co., Amsterdam, the Netherlands, 1973.
6. J. S. Shah in B. R. Pamplin, ed., *Crystal Growth*, Pergamon, Oxford, U.K., 1975, Chapt. 4.
7. W. Keller and A. Mühlbauer, *Floating-Zone Silicon*, Marcel Dekker, Inc., New York, 1981.
8. W. R. Wilcox, *CHEMI Module SMT-50*, American Institute of Chemical Engineers, in press.
9. M. Chang and R. Kennedy, *J. Electrochem. Soc.* **128**, 2193 (1981).
10. G. R. Atwood, *Chem. Eng. Prog. Symp. Ser.* **65**, 112 (1969).
11. A. M. Nazar and T. W. Clyne in T. N. Veziroglu, ed., *Proceedings Multi-Phase Flow and Heat Transfer Symposium*, Hemisphere, Washington, D.C., 1980.
12. N. W. Lord, *Trans. AIME* **197**, 1531 (1953).
13. W. R. Wilcox, *Sep. Sci. Technol.* **17**, 1117 (1982).
14. L. Burris, Jr., C. H. Stockman, and I. G. Dillon, *Trans. AIME* **203**, 1017 (1955).
15. E. Helfand and R. L. Kornegay, *J. Appl. Phys.* **37**, 2484 (1966).
16. I. Brown, *Brit. J. Appl. Phys.* **8**, 457 (1957).
17. J. R. Gould, *Trans. AIME* **221**, 1154 (1961).
18. Sh. I. Peizulaev, *Inorg. Mater.* **3**, 1329 (1967).
19. G. Matz, *Chem. Ing. Techn.* **4**, 381 (1964); Sh. I. Peizulaev, *Inorg. Mater.* **3**, 1329 (1967).
20. B. V. Ramarao, W. R. Wilcox, and W. E. Briggs, *J. Cryst. Growth* **59**, 557 (1982).
21. P. S. Ravishankar and W. R. Wilcox, *J. Cryst. Growth* **43**, 480 (1978).
22. H. M. Yeh and W. H. Yeh, *Sep. Sci. Technol.* **14**, 795 (1979).
23. D. Fischer, *J. Appl. Phys.* **44**, 1977 (1973).
24. J. A. Burton, R. C. Prim, and W. P. Slichter, *J. Chem. Phys.* **21**, 1987 (1953).
25. W. R. Wilcox, *Mater. Res. Bull.* **4**, 265 (1969).
26. W. R. Wilcox, *J. Appl. Phys.* **35**, 636 (1964).
27. J. R. Carruthers in W. R. Wilcox and R. A. Lefever, eds., *Preparation and Properties of Solid State Materials*, Vol. 3, Marcel Dekker, Inc., New York, 1977, Chapt. 1.

28. J. R. Carruthers, *J. Cryst. Growth* **32**, 13 (1976).
29. W. R. Wilcox and L. D. Fullmer, *J. Appl. Phys.* **36**, 2201 (1965).
30. M. A. Azouni, *J. Cryst. Growth* **47**, 109 (1979).
31. H. C. Gatos and A. F. Witt in A. Bishay, ed., *Recent Advances in Science and Technology of Materials*, Vol. **1**, Plenum Publishing Corp., New York, 1973.
32. W. R. Wilcox, *Sep. Sci.* **2**, 411 (1967).
33. S. Sen, R. A. Lefever, and W. R. Wilcox, *J. Cryst. Growth* **43**, 526 (1978).
34. W. R. Wilcox and S. Sen, *Mater. Res. Bull.* **13**, 293 (1978).
35. H. P. Utech and M. C. Flemings, *J. Appl. Phys.* **37**, 2021 (1966).
36. A. F. Witt, C. J. Herman, and H. C. Gatos, *J. Mater. Sci.* **5**, 822 (1970).
37. W. R. Wilcox, *Mater. Res. Bull.* **2**, 121 (1967).
38. J. C. Brice, *J. Cryst. Growth* **28**, 249 (1975).
39. V. V. Voronkov and A. A. Chernov, *Sov. Phys.-Crystallogr.* **12**, 186 (1967).
40. D. E. Temkin, *Sov. Phys.-Crystallogr.* **17**, 405 (1972).
41. J. D. Weeks and G. H. Gilmer, *Adv. Chem. Phys.* **40**, 157 (1979).
42. H. Pfeiffer, *J. Cryst. Growth* **52**, 350 (1981).
43. J. C. Brice, *J. Cryst. Growth* **10**, 205 (1971).
44. W. A. Tiller and K.-S. Ahn, *J. Cryst. Growth* **49**, 483 (1980).
45. R. F. Sekerka in P. Hartman, ed., *Crystal Growth: An Introduction*, North-Holland Publishing Co., Amsterdam, the Netherlands, 1973, Chapt. 15.
46. D. J. Wollkind in W. R. Wilcox, ed., *Preparation and Properties of Solid State Materials*, Vol. **4**, Marcel Dekker, Inc., New York, 1979, Chapt. 4.
47. S. R. Coriell and R. F. Sekerka, *J. Cryst. Growth* **34**, 157 (1976).
48. J. S. Langer, *Acta Met.* **25**, 1121 (1977).
49. T. Sato, K. Shibata, and G. Ohira, *J. Cryst. Growth* **40**, 69 (1977).
50. D. E. Temkin, *Sov. Phys. Crystallogr.* **22**, 529 (1977).
51. W. W. Mullins and R. F. Sekerka, *J. Appl. Phys.* **35**, 444 (1964).
52. A. L. Conlet, B. Billia, and I. Capella, *J. Cryst. Growth* **51**, 106 (1981).
53. S. R. Coriell, M. R. Cordes, W. J. Boettinger, and R. F. Sekerka, *J. Cryst. Growth* **49**, 13 (1981).
54. S. R. Coriell, D. T. J. Hurle, and R. F. Sekerka, *J. Cryst. Growth* **32**, 1 (1976).
55. D. E. Holmes and H. C. Gatos, *J. Appl. Phys.* **52**, 2971 (1981).
56. J. P. Dismukes and W. M. Yim, *J. Cryst. Growth* **22**, 287 (1974).
57. D. J. Morantz and K. K. Mathur, *J. Cryst. Growth* **16**, 147 (1972).
58. J. Verhoeven, *Met. Trans.* **2**, 2673 (1971).
59. D. D. Edie and D. J. Kirwan, *Ind. Eng. Chem. Fundam.* **12**, 100 (1973).
60. B. Ozum and D. J. Kirwan, *AIChE Symp. Ser.* **72**(153), 1 (1976).
61. N. Streat and F. Weinberg, *Met. Trans.* **7B**, 417 (1976).
62. A. A. Chernov, D. E. Temkin, and A. M. Mel'nikova, *Sov. Phys. Crystallogr.* **21**, 652 (1976).
63. S. N. Omenyi and A. W. Neumann, *J. Appl. Phys.* **47**, 3956 (1976).
64. R. R. Gilpin, *J. Colloid Int. Sci.* **74**, 44 (1980).
65. P. F. Aubourg, *Interaction of Second Phase Particles with Crystal Growing from Melt*, Ph.D. thesis, MIT, Cambridge, Mass., 1978.
66. J. E. Coon and W. R. Wilcox, *Sep. Sci. Technol.* **15**, 1401 (1980).
67. R. B. Fedich and W. R. Wilcox, *Sep. Sci. Technol.* **15**, 31 (1980).
68. W. R. Wilcox, *Sep. Sci.* **4**, 95 (1969).
69. C. E. Chang and W. R. Wilcox, *J. Cryst. Growth* **21**, 182 (1974).
70. N. Kobayashi, *J. Cryst. Growth* **43**, 417 (1978).
71. A. R. McGhie, P. J. Rennolds, and G. J. Sloan, *Anal. Chem.* **52**, 1738 (1980).
72. N. J. G. Bollen, M. J. Van Essen, and W. M. Smit, *Anal. Chim. Acta* **38**, 279 (1967).
73. G. J. Sloan, *Mol. Cryst.* **1**, 161 (1966).
74. K. D. Wolter, P. L. Carella, G. A. Moebus, and J. F. Johnson, *Sep. Sci. Technol.* **14**, 805 (1979).
75. I. N. Anikin and Kh. S. Bagdasarov, *Sov. Phys. Crystallogr.* **25**, 81 (1980).

76. P. A. Clark and W. R. Wilcox, *J. Cryst. Growth* **50**, 461 (1980).
77. C. E. Chang, W. R. Wilcox, and R. A. Lefever, *Mater. Res. Bull.* **14**, 527 (1979).
78. D. Schwabe and A. Scharmann, *J. Cryst. Growth* **46**, 125 (1979).
79. *Ibid.*, **52**, 435 (1981).
80. Ch.-H. Chun, *J. Cryst. Growth* **48**, 600 (1980).
81. W. R. Wilcox, R. S. Subramanian, J. M. Papazian, H. D. Smith, and D. M. Mattox, *AIAA J.* **17**, 1022 (1979).
82. B. K. Jindal, *J. Cryst. Growth* **16**, 280 (1972).
83. O. V. Abramov, I. I. Teumin, V. A. Filonenko, and G. I. Eskin, *Sov. Phys. Acoust.* **13**, 141 (1967).

WILLIAM R. WILCOX
Clarkson College of Technology

Related Articles

Crystallization; Mass transfer